

Study of structural, morphological and optical properties of nanostructured Zirconium doped V₂O₅ thin films

T Akkila^{1*}, I Mansur Basha^{1,2}

¹PG& Research Department of Physics, Govt. Arts College, Trichy-620 022, Tamilnadu

²PG& Research Department of Physics, Jamal Mohamed College (Autonomous), Trichy-620 020, Tamilnadu
Email: akkilaprofes@gmail.com

Abstract- Thin films of zirconium doped vanadium pentoxide with different Zr-doping levels (in steps of 0.1mM of Zr) were deposited on glass substrates by a home built spray pyrolysis system. The effect of Zr doping on the structural, morphological and optical characteristics were carried out. X – ray diffraction (XRD) patterns revealed that prepared films were polycrystalline in nature, having an orthorhombic crystal structure. Annealing effect improved the crystallinity of the films. The crystallite size of the films was found to increase after annealing. From FESEM images, the flower shaped structure was observed in the annealed Zr doped V₂O₅ film. The band gap energy of as deposited films varied with Zr doping.

Index Terms- thin films; Spray pyrolysis; X –ray diffraction; Zirconium dopant.

1. INTRODUCTION

Doping metal oxides has been utilized as one method for enhancing or changing the properties of the oxides for new and upgraded execution of different electronic devices. Transition metals specifically introduce changes in electrical, structural, optical and morphological characteristics of the parent metal oxides. V₂O₅ continuously studied due to its potential for many applications such as optical switching devices [1], humidity sensors, secondary Li batteries and electrochromic materials [2]. The relationship between microscopic and macroscopic properties, materials, and deposition parameters provides an important guidance to optimize these material characteristics for a given application [3]. V₂O₅ films have been prepared by a various physical and chemical vapor deposition techniques such as chemical vapor deposition [4] sputtering [5], sol gel method [6], pulsed laser deposition [6], evaporation [7-9] and spray pyrolysis [10, 11].

Introduction of Zr atoms as dopants into the V – O matrix has been studied in the form of nanoparticles [12, 13], thin films [14]. Interest in Zr doped V₂O₅ arises from the fact that wide band gap of ZrO₂ is beneficial to widen the bandgap and potential to increase the absorbance. The molecular mixing of these components is vital in transforming the properties of the mixed oxides. Changes in their properties caused by doping usually depend on the synthesis method and conditions, the ratios of the components, nature of source materials and post-synthesis treatments. The main objective of this study was to deposit undoped and Zr-doped V₂O₅ thin films using the spray pyrolysis method and to investigate the effect of doping on their structural, morphological and optical properties.

2. EXPERIMENTAL

2.1. Preparation of Zn-Doped V₂O₅ Thin Films

Vanadium (III) chloride (Sigma-Aldrich, USA, purity 99.8%) and Zirconium oxychloride, (Sigma-Aldrich, USA, purity 98%) were used as sources of vanadium and zirconium oxides respectively. Initially, for pristine V₂O₅ thin film 0.05M of vanadium (III) chloride (VCl₃) was dissolved in 50 mL of deionized water. For Zr doped V₂O₅, an appropriate quantity of Zirconium oxychloride (ZrOCl₂.8H₂O) was added from 0.1mM to 0.5mM in steps of 0.1mM in the precursor solution respectively. The solution was stirred thoroughly using a magnetic stirrer for 30 min and then deposited on the preheated glass substrates kept at 250°C by spray pyrolysis system. A home built spray system was constructed as reported by Jeyaprakash et al [17].

Before the deposition process, the glass substrates were cleaned chemically and dried to remove the unwanted organic matters present in the substrate. The cleaned glass substrates were placed on the heater which is controlled by chrome-nickel thermocouple fed to a temperature controller with an accuracy of ±1°C. The solution was sprayed at an angle of 45° onto preheated glass substrate kept at a distance of 50cm from the spray gun. Compressed dry air at a pressure of 2 kg/cm² by an air compressor via an air filter with regulator was employed as the carrier gas and spray rate of the solution was kept at 3 ml/min. To avoid excessive cooling of substrates, consecutive spraying process was employed with the time period of 15 seconds between two sprays. All the prepared film samples were post annealed at 300°C for 1 hour in an air atmosphere.

2.2. Characterization techniques

The structural details of the thin films prepared by the afore mentioned process, were carried out by P Analytical X-ray diffractometer (Model D/MAX ULTIMA III) using Ni – filtered CuK α X- radiation ($k=1.54056\text{\AA}$). A range of 2θ from 10° to 100° was scanned from a fixed slit type so that all possible diffraction peaks could be detected. Crystallite size and micro strain were analyzed by X-Ray line broadening technique. Surface morphology of the films was investigated using Field Emission Scanning Electron Microscope (Model Carl Zeiss Ultra 55) with an accelerating potential of 18KV. Prior to the imaging, the films were sputtered with a thin gold film to increase the emission of the secondary electron for enhanced imaging. All the spectra were acquired at a pressure using an ultra-high vacuum with Al Ka excitation at 250W. The optical properties and the band gap of the thin films were analyzed by UV-VIS-NIR spectrophotometer (Model- Lambda 35).

3. RESULTS AND DISCUSSION

3.1. Structural Analysis

To study the crystalline structure and phase change in the prepared samples before and after heat treatment, XRD has been performed as shown in figure 1. The XRD pattern of as deposited pristine V_2O_5 film corresponded with the orthorhombic structure (JCPDS 41-1426) while the impurity peak due to V_4O_9 . However, the XRD pattern of the pristine V_2O_5 had low peak intensities because of the poor crystallinity. Zr as dopant suppressed the crystal growth of V_2O_5 along (0 0 1) direction and increasing the intensity along (1 0 1) plane. The peak intensity increased gradually with increase of dopant concentration. These results conclude that, Zr^{4+} is well doped within the V_2O_5 lattice.

As it can be seen, with open air annealing at 300°C crystallinity of the films were improved. Fig 2 (b) exhibits typical V_2O_5 phase with major peaks along (0 0 1), (2 0 0) and (1 1 0). The observed pattern is in accordance with the previous work prepared by the spray pyrolysis and other methods [11, 15 - 16]. At higher concentration of Zr (0.5mM), (0 0 1) peak becomes dominant. The dominance of (0 0 1) peak suggests that the texture of V_2O_5 thin film is oriented along c – axis which is perpendicular to the surface of the substrate with it's a- , b- axis parallel to the surface [17]. The crystallite size and microstrain were calculated using Scherrer's formula [18],

$$D = 0.9\lambda / \beta \cos\theta \text{ and}$$

$$\epsilon_{hkl} = \beta/4\tan\theta$$

Where D is the size of the grain in the direction perpendicular to the reflecting planes, θ is diffraction angle, K is shape factor ($=0.9$), λ is the wavelength of

X-ray, β is the full width at half maximum of prominent peaks in radian and ϵ_{hkl} is microstrain. Figure 3(a) and 3(b) show the variation of mean crystallite size and microstrain for both as deposited and annealed films. It is observed that the crystallite size decreases with dopant concentration increases. It is mainly due to change in peak position with Zr doping. After annealing, the crystallite size was found to increase due to coalescence process [19]. The grain orientations as a function of Zr concentration as shown in figure 4. The peak intensity $I(101)/I(001)$ is mapped for various Zr concentration for as deposited films. For low Zr concentration, (0 0 1) peak shows the highest peak intensity and the (1 0 1) the second highest ($I(101)/I(001) > 1$). At higher concentration of Zr, (1 0 1) peak dominates with respect to the (0 0 1) reflection ($I(101)/I(001) < 1$) as the (1 0 1) peak intensity increases rapidly in contrast to the intensity of the (0 0 1) peak. With post annealing, microstrain decreases due to ordering of atoms in the crystal lattice and concentration of stacking faults and point defects are reduced [20].

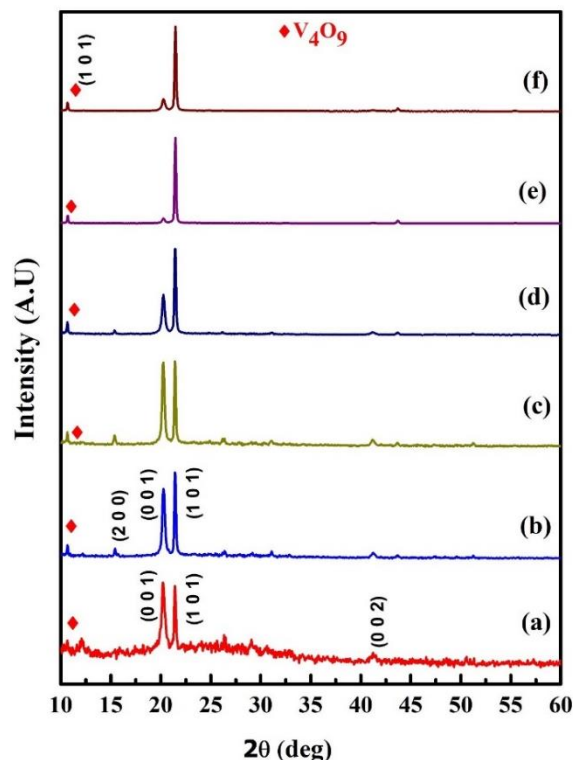


Fig 1: XRD patterns of as deposited (a) Pristine V_2O_5 and Zr doped (b) 0.1 mM (c) 0.2 mM (d) 0.3 mM (e) 0.4 mM (f) 0.5 mM. V_2O_5 thin film

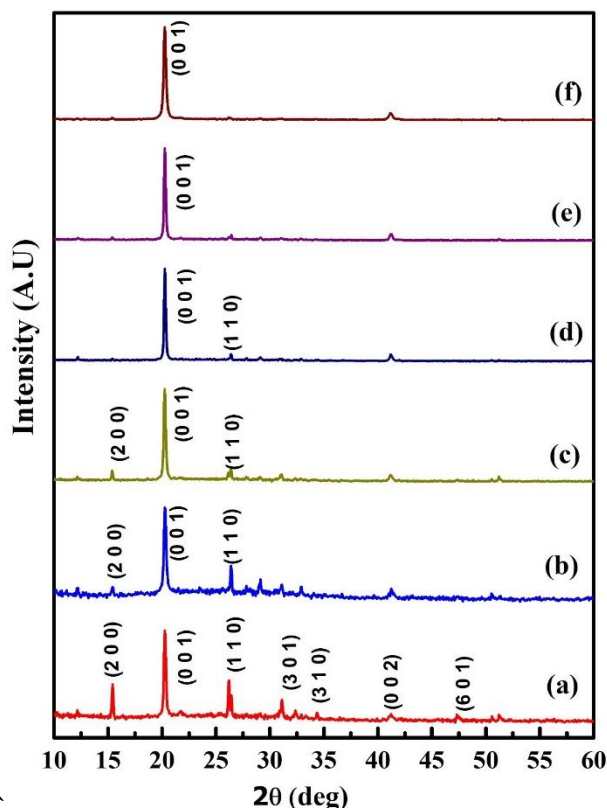


Fig 2: XRD patterns of annealed (a) Pristine V_2O_5 and Zr doped (b) 0.1 mM (c) 0.2 mM (d) 0.3 mM (e) 0.4 mM (f) 0.5 mM V_2O_5 thin films

3.2. Morphological Analysis

The surface morphology of the as deposited and annealed films was studied using FESEM images shown in Figure. 5 – 7. As deposited pristine and Zr doped thin films show smooth and tightly packed grains with some fine pores. As observed in Figure 5, there is a noticeable difference between as deposited and annealed films. While annealing the agglomeration process is initiated resulting in the formation of larger grains. In contrast to the as deposited pristine V_2O_5 film, the annealed V_2O_5 film presents a slightly coherent and homogeneous morphology, consisting of flower shaped morphology (Figure 6 – b). It is attributed to the migration of surface atoms at higher temperatures. In addition, more voids were observed among Nano flowers. Figure 7 shows the structure of Nano flowers with different magnification. Nano flowers with the porous nature of the film which is useful for the solar cell and sensor application. [21]. Thus the higher concentration of Zr doping affect the crystal structure and morphology of V_2O_5 thin films

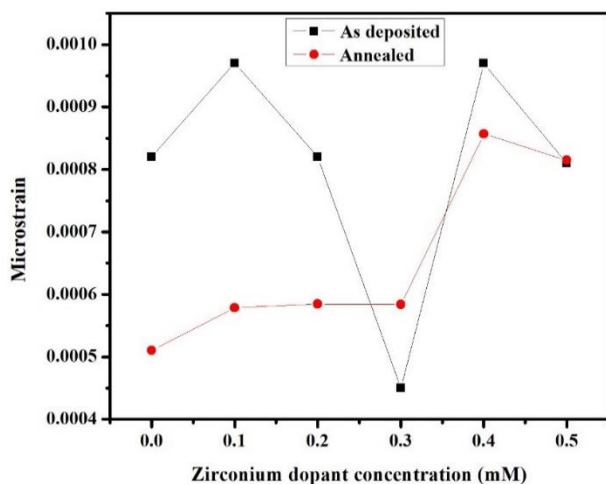
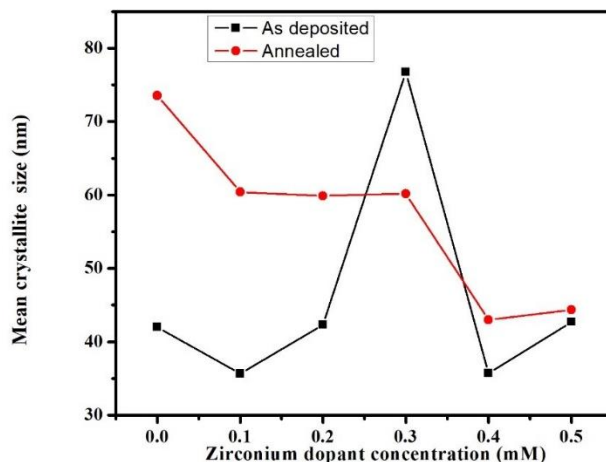


Fig 3: Variation of (a) Mean crystallite size and (b) microstrain of as deposited and annealed Pristine and Zr doped V_2O_5 thin films

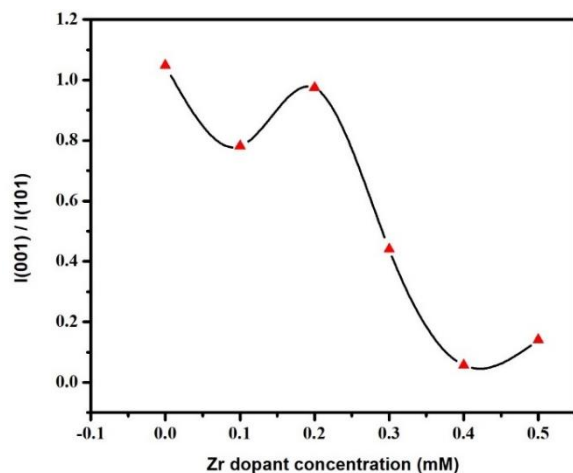


Fig 4: Grain orientations as a function of Zr concentration

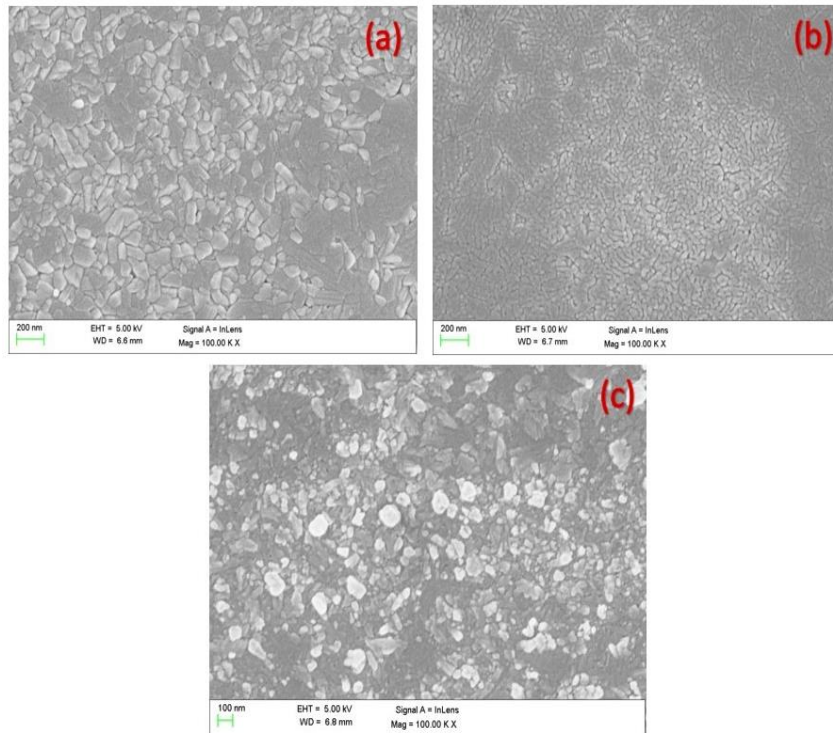


Fig. 5: FESEM images of as deposited (a) and Zr doped with 0.3(b) and 0.5mM (c)

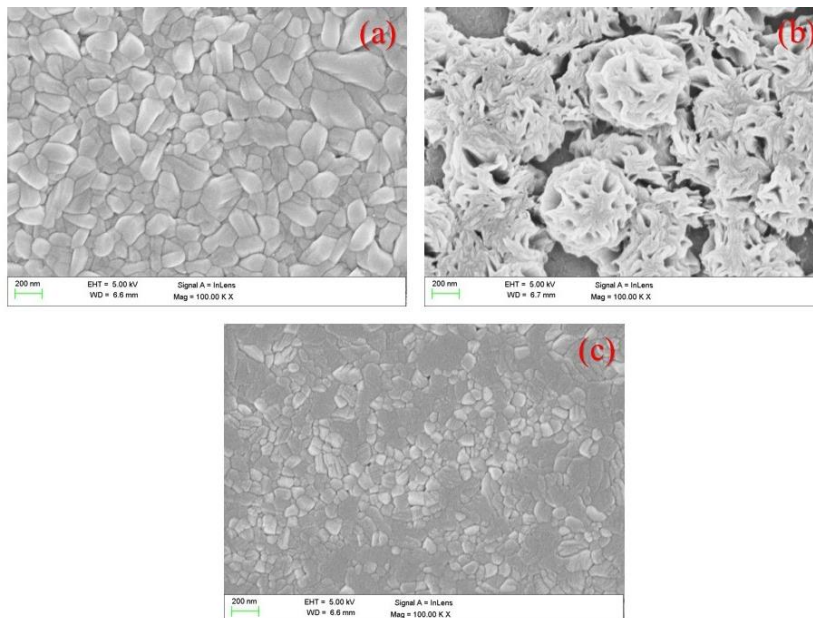


Fig 6: FESEM images of annealed pristine V_2O_5 (a) and Zr doped with 0.3(b) and 0.5mM (c)

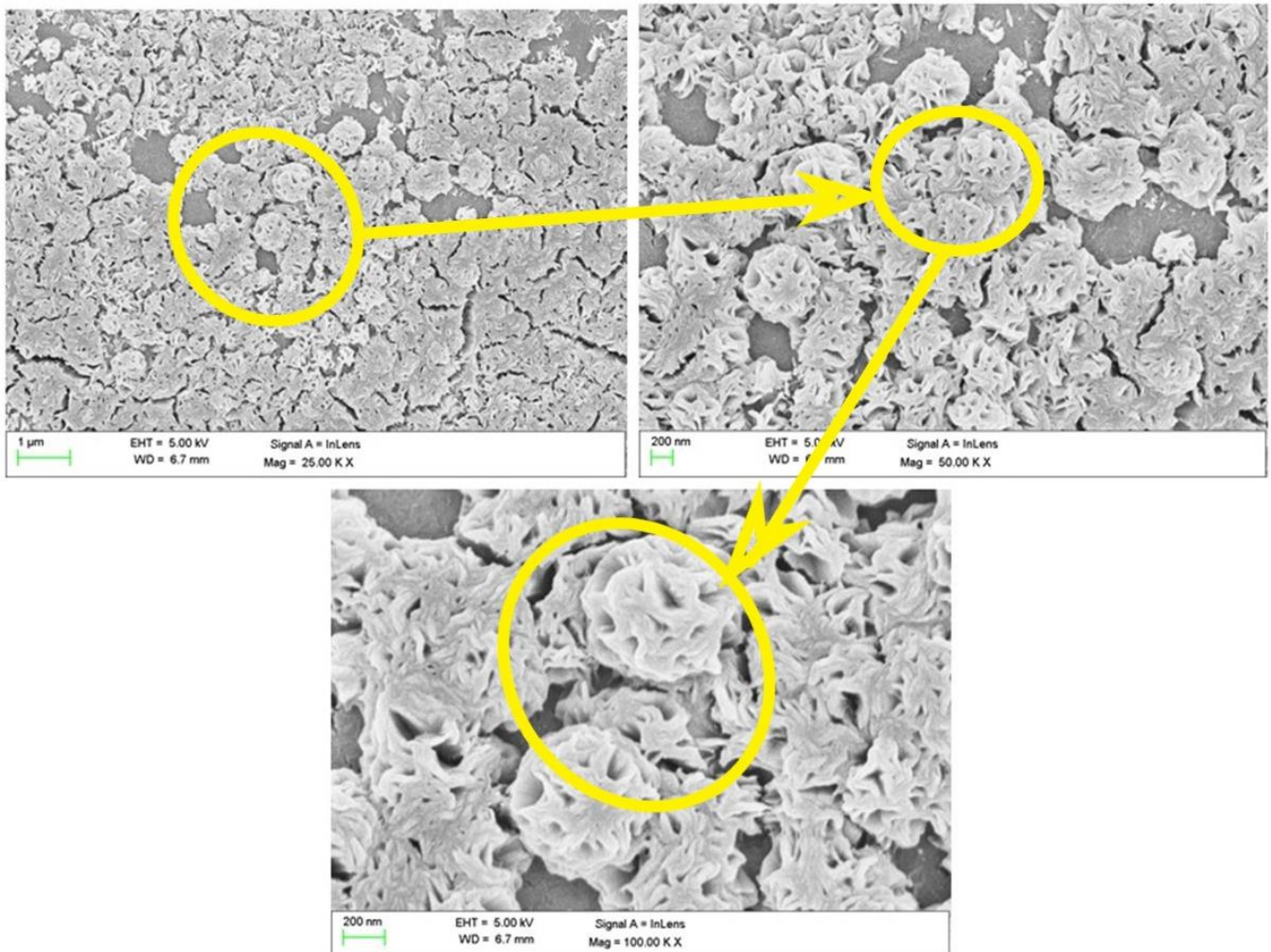


Fig 7: FESEM images of annealed pristine V_2O_5 (a) and Zr doped with 0.3(b) and 0.5mM (c)

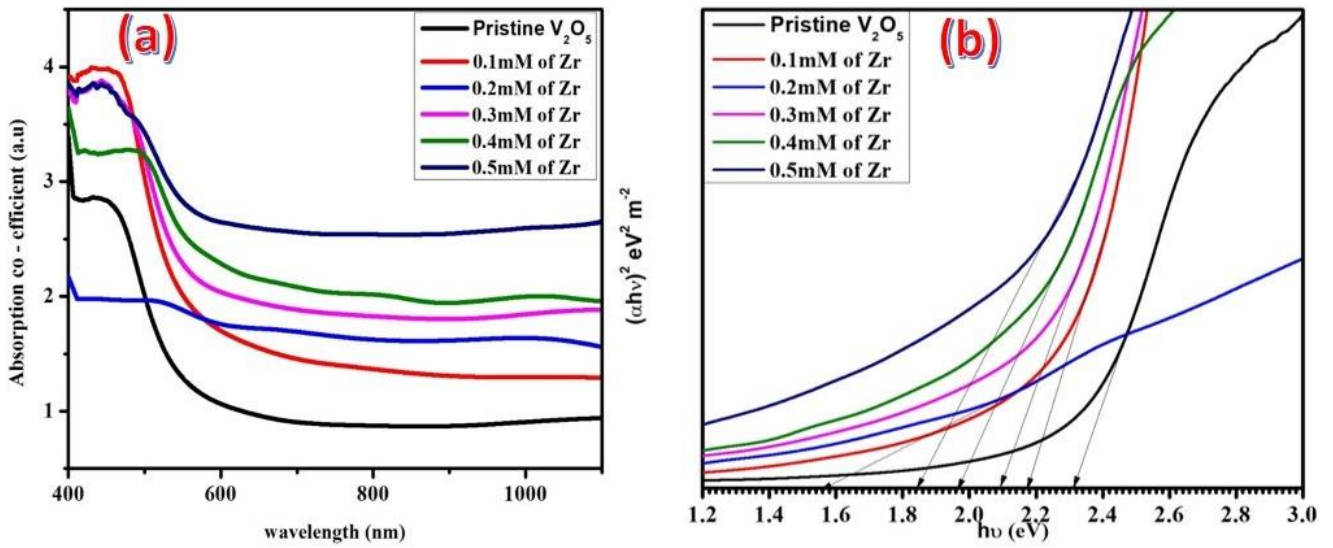


Fig 8: Absorbance spectra (a) and Tauc's plot (b) of as deposited V_2O_5 thin films doped d with different Zr concentrations

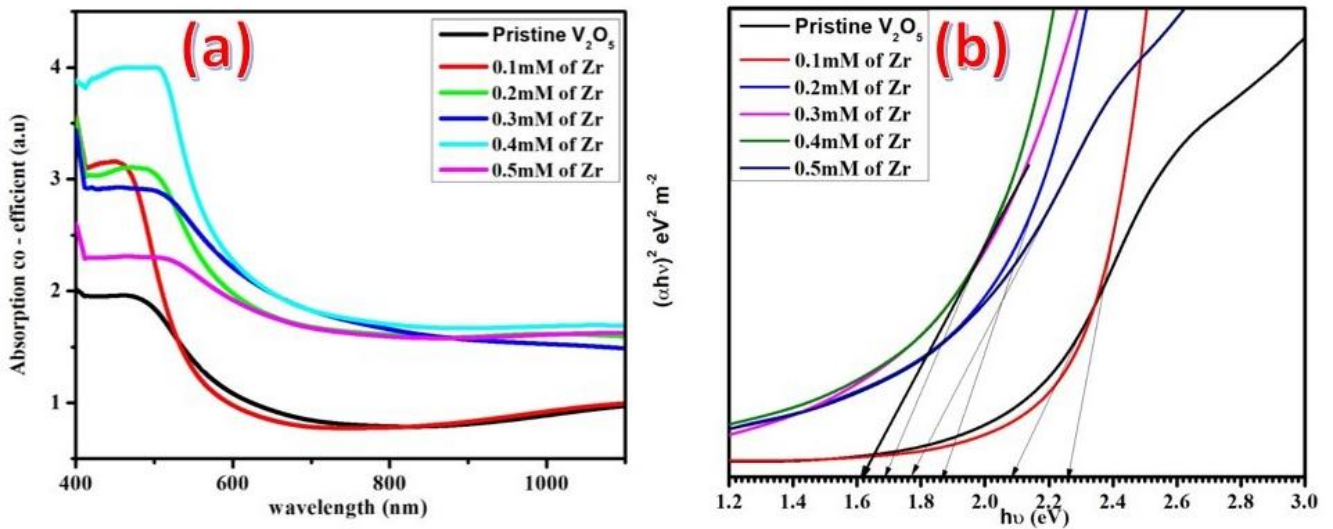


Fig 9: Absorbance spectra (a) and Tauc's plot (b) of annealed V_2O_5 thin films doped with different Zr concentrations

3.3. Optical studies

Figure 8 and 9 show the optical absorption spectra and Tauc's plot of as deposited and annealed pristine V_2O_5 and Zr - doped V_2O_5 thin films. Generally, by increasing the dopant concentration, the optical absorbance increases intensely. The absorbance of the Zr-doped V_2O_5 films decreases as the Zr-doping level increases from 0.1mM to 0.4mM except 0.2mM concentration. This rise in absorption edge is the result of the decreased band gap which improves the thin film conducting behavior. However this trend is reversed for 0.2mM dopant concentration which is probably resulted from more porosity in film. The absorbance decreased considerably with post annealing at 300°C. The optical absorption coefficient ' α ' was estimated by the following relation:

$$\alpha = 2.303A / t$$

Where A is the absorbance and t is the thickness of the film. The optical band gap was calculated using Tauc's relation [22],

$$(\alpha h\nu)^{1/n} = B (h\nu - E_g)$$

Where $h\nu$ is the photon energy, E_g is the cortical band gap of the film, α is the absorption coefficient, 'B' is constant, the exponent 'n' corresponding to the type of transition. The values of n - 1/2, 2, 3/2 and 3, correspond to the allowed indirect, direct, forbidden direct band gaps indirect and forbidden respectively.

The optical band gap energies of as - deposited pristine V_2O_5 are 2.32eV which is in agreement with the previous works [23]. As the doping concentration increases, the band gap energy found to decrease. The lowering band gap is related to the grain size [24]. When the prepared samples are annealed at 300°C, the energy gap is shifted to lower energy and it clearly indicates that the annealing processes decreases band gap energy. The microstructural changes caused by annealing treatment can be attributed to decrease in optical band gap [25, 26]. The effect of grain size on the optical band gap arises out of quantum confinement effects [26]. The variations of E_g with Zn doping concentration of both as deposited and annealed films are shown in figure 10.

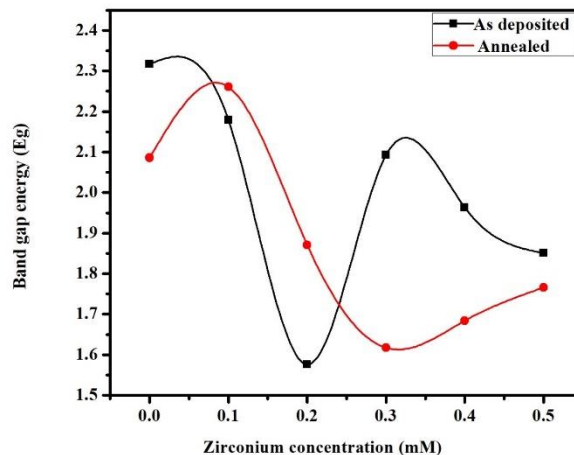


Fig 9: Absorbance spectra (a) and Tauc's plot (b) of annealed V_2O_5 thin films doped with different Zr concentrations

Conclusion

In this work, we investigate the effect of Zr-doping of different levels on the physical properties of vanadium oxide thin films prepared by spray pyrolysis. Our results revealed that Zr-doping in vanadium oxide thin films strongly affects its physical properties. The X - ray diffractometry showed that films were polycrystalline nature with orthorhombic structure. By increasing the level of doping suppressed the crystal growth of V_2O_5 along (0 0 1) direction and increased the intensity along (1 0 1) plane. After annealing, (0 0 1) plane become dominated. The SEM micrographs show that formation of Nano flowers in annealed Zr doped V_2O_5 thin films. UV - Vis spectra illustrated that the doping samples with zirconium decreased the band gap of the films. With annealing, the band gap energy values found to decrease and it is attributed due to structural changes in the films.

REFERENCES

- [1] Bnenmoussa, A. Outzourhit, A. Bennouna, E.L. Ameziane, Electrochromism in sputtered V_2O_5 thin films: structural and optical studies, Thin Solid Films, 405 (2002) 11 - 16
- [2] J.P. Pereira-Ramos, R. baddour, S. Bach, N. Baffer, Electrochemical and structural characteristics of some lithium intercalation materials synthesized via a sol-gel process: V_2O_5 and manganese dioxides-based compounds, Solid State Ionics, 53/56 (1992) 701 - 709.
- [3] E. Potiron, A. Le Gal, la Salle, A. Verbaere, Y. Piffard, D. Guyomard, Electrochemically synthesized vanadium oxides as lithium insertion hosts, Electrochimica Acta, 45 (1999) 197 - 214.

- [4] B. N. B. Thi, T. P. Minh, B. Simona, Optical and electrochemical properties of vanadium pentoxide gel thin films, *J. Appl. Phys.* 80 (1996) 7041.
- [5] L. Ottaviano, A. Pennisi, F. Simone, A.M. Salvi, RF sputtered electrochromic V_2O_5 films *Opt. Mater.* 27 (2004) 307 – 313
- [6] N. Ozcr, Electrochemical properties of sol-gel deposited vanadium pentoxide films, *Thin Solid Films* 305 (1997) 80
- [7] M.F. Al-Kuhaili, E.E. Khawaja, D.C. Ingram, S.M.A. Durrani, A study of thin films of V_2O_5 containing molybdenum from an evaporation boat, *Thin Solid Films* 460 (2004) 30 – 35
- [8] R.T. Rajendra Kumar, B. Karunakaran, V. Senthil Kumar, Y.L. Jcyachandran, D. Mangalaraj, S.K. Narayandas, Structural properties of V_2O_5 thin films prepared by vacuum evaporation, *Mater. Sci. Semicond. Process.* 6 (2003) 543 – 546
- [9] C.V. Ramana, O.M. Hussain, Naidu B. Srinivasalu, C. Julien, M. Balkanski, *Mater. Sci. Eng., B, Solid-State Mater. Adv. Technol.* 52 (1998) 32.
- [10] A.A. Akl, Thermal annealing effect on the crystallization and optical dispersion of sprayed V_2O_5 thin films, *J. Phys. Chem. Solids* 71 (2010) 223 – 229
- [11] R. Irani. S.M. Rozati, S. Beke, Structural and optical properties of nanostructural V_2O_5 thin films deposited by spray pyrolysis technique: Effect of the substrate temperature, *Mater. Chem. Phys.* 139 (2013) 489 – 493.
- [12] N. Shen, S. Chen, Z. Chen, X. Liu, C. Cao, B Dong, H Luo, J. Liua, Y Gao, The synthesis and performance of Zr-doped and W–Zr-codoped VO_2 nanoparticles and derived flexible foil, *J. Mater. Chem. A*, (2014) 2, 15087.
- [13] Y N Ko, S H Choi, Y C Kang, and S B Park, *Appl. Mater. Interfaces* 5, (2013) 3234–3240.
- [14] H. Zhang, Z. Wu, X. Wu, X Wei, Y. Jiang, Preparation and phase transition properties of nanostructured zirconium-doped vanadium oxide films by reactive magnetron sputtering, *Thin solid films* 568 (2014) 63 – 69.
- [15] Y. Vijayakumar, G.K. Mani, M.V. Ramana Reddy, J.B.B. Rayappan, Nanostructured flower like V_2O_5 thin films and its room temperature sensing characteristics, *Ceram. Int.* 41 (2015) 2221 – 2227.
- [16] Z.S. El Mandouh, M.S. Selim, Physical properties of vanadium pentoxide sol gel films, *Thin Solid Films* 371 (2000) 259 – 263.
- [17] A. Kumar, P. Singh, N. Kulkarni, D. Kaur, Structural and optical studies of nanocrystalline V_2O_5 thin films, *Thin solid films* 516 (2008) 912 – 918.
- [18] A. L. Patterson, The Scherrer Formula for X-Ray Particle Size Determination, *Phy. Rev.* 56 (1939) 978 (1939).
- [19] M Indumathy, G K Mani, P Shankar, J B B Rayappan, Effect of nickel doping on structural, optical, electrical and ethanol sensing properties of spray deposited nanostructured ZnO thin films, *Ceram. Int.* 40 (2014) 7993 – 8001.
- [20] J L M Rupp, A Infortuna, L J Gauckler, Microstrain and self-limited grain growth in nanocrystalline ceria ceramics, *Acta Materialia* 54 (2006) 1721–1730.
- [21] C. M. Muvia, T.S. sathiyaraj, K. Maabong, effect of doping concentration on the properties of aluminium doped Zinc oxide thin films prepared by spray pyrolysis for transparent electrode applications, *Cerm .int* 37 (2011) 555 – 560 .
- [22] M M Bagheri-Mohagheghi, N Shahtahmasebi, M R Alinejad, A Youssefi and M Shokooh-Saremi, The effect of the post-annealing temperature on the nano-structure and energy band gap of SnO_2 semiconducting oxide nano-particles synthesized by polymerizing–complexing sol–gel method, *Physica B* 403 (2008) 2431 – 2437.
- [23] S.F Cogan, N M Nguyen, S.J Perrotti, R D Rauh, Optical properties of electrochromic vanadium pentoxide, *Journal of Applied Physics* 66 (1989) 1333 – 1337.
- [24] Ramana C V, Smith R J, Hussain O M, Chusuei C C and Julien C M 2005 *Chem. Mater.* 17 1213
- [25] D. Vasanth Raj, N. Ponpandian, D. Mangalaraj, C. Viswanathan, Effect of annealing and electrochemical properties of sol-gel dip coated nanocrystalline V_2O_5 thin films, *Mater. Sci. Semicond. Process.* 16 (2013) 256 – 262.
- [26] Yu, I., T. Isobe, M. Seena, *Mater. Res. Bull.* 30, 75 (1995)